Eur Respir J 2010; 36: 311–322
DOI: 10.1183/09031936.00122509

Identification of a novel water-soluble activator of wild-type and F508del CFTR: GPact-11a

J. Bertrand*, B. Boucherle#, A. Billet*, P. Melin-Heschel*, L. Dannhoffer*, C. Vandebrouck*, C. Jayle¶, C. Routaboul#, M-C. Molina#, J-L. Décout#, F. Becq* and C. Norez*

ABSTRACT: One of the major therapeutic strategy in cystic fibrosis aims at developing modulators of cystic fibrosis transmembrane conductance regulator (CFTR) channels. We recently discovered methylglyoxal α-aminoazaheterocycle adducts, as a new family of CFTR inhibitors. In a structure–activity relationship study, we have now identified GPact-11a, a compound able not to inhibit but to activate CFTR.

Here, we present the effect of GPact-11a on CFTR activity using *in vitro* (iodide efflux, fluorescence imaging and patch-clamp recordings), *ex vivo* (short-circuit current measurements) and *in vivo* (salivary secretion) experiments.

We report that GPact-11a: 1) is an activator of CFTR in several airway epithelial cell lines; 2) activates rescued F508del-CFTR in nasal, tracheal, bronchial, pancreatic cell lines and in human CF ciliated epithelial cells, freshly dissociated from lung samples; 3) stimulates *ex vivo* the colonic chloride secretion and increases *in vivo* the salivary secretion in *cftr*$^{+/+}$ but not *cftr*$^{-/-}$ mice; and 4) is selective for CFTR because its effect is inhibited by $CFTR_{inh}$-172, GlyH-101, glibenclamide and GPinh-5a.

To conclude, this work identifies a selective activator of wild-type and rescued F508del-CFTR. This nontoxic and water-soluble agent represents a good candidate, alone or in combination with a F508del-CFTR corrector, for the development of a CFTR modulator in cystic fibrosis.

KEYWORDS: Airway epithelial cells, cystic fibrosis, epithelial ion transports, F508del-CFTR activator, knock-out mice, methylglyoxal-9-propyladenine

The cystic fibrosis transmembrane conductance regulator (CFTR) protein is a cAMP-dependent and ATP-gated chloride channel, localised at the apical surface, mediating Cl^- transepithelial transport in airways, intestine and other fluid transporting tissues [1–4]. Defective function of CFTR is responsible for cystic fibrosis (CF), one of the most common, lethal autosomal recessive human disorders in Caucasians. The principal clinical problem in CF is recurrent lung infections, resulting in progressive lung deterioration. More than 1,500 mutations in *CFTR* have been identified that cause CF phenotypes, with ~90% of CF patients having the F508del mutation in one or both *CFTR* alleles. The deletion of F508 induces a trafficking- and gating-defect of CFTR protein leading to an impaired channel activity even when present at the cell plasma membrane [5].

In developing chloride-channel enhancement therapy for CF, it is assumed that restoring Cl^- permeability would correct the underlying cellular defect that causes lung disease. Therefore, searching for reagents modifying the activity of CFTR is an active area of research and one of the major therapeutic strategies in CF. A number of pharmacological agents able to potentiate the cAMP-dependent CFTR function have been identified [6, 7] and are termed ''potentiators'' (for example genistein, VX-770, alkylxanthines). Moreover, some classes of potentiators, although being very potent on wild-type (wt) CFTR, have limited efficacy on F508del-CFTR mutants, such as forskolin (Fsk), β2-adrenergic or A2B-adenosine receptor agonists [6, 8, 9], some of them lack selectivity [6, 10] and have low affinity [11, 12]. Another class of CFTR modulators, called ''activators'' of CFTR, were selected on the basis of their potency (low micromolar to submicromolar range) and their ability to induce CFTR-dependent electrogenic Cl^- transport in a way independent of cAMP.

AFFILIATIONS
*Institut de Physiologie et Biologie Cellulaires, Université de Poitiers, CNRS,
¶Service de Chirurgie Cardiothoracique, CHU La Milétrie, Poitiers, and
#Département de Pharmacochimie Moléculaire, Université de Grenoble, CNRS, Grenoble, France.

CORRESPONDENCE
C. Norez
Institut de Physiologie et Biologie Cellulaires
Université de Poitiers
CNRS UMR 6187
40 Avenue du Recteur Pineau
86022 Poitiers
France
E-mail: caroline.norez@univ-poitiers.fr

Received:
July 31 2009
Accepted after revision:
Jan 12 2010
First published online:
Jan 28 2010

European Respiratory Journal
Print ISSN 0903-1936
Online ISSN 1399-3003

In a previous study, we described a new family of CFTR inhibitors: the methylglyoxal α-aminoazaheterocycle adducts; among them, the nucleoside 5a (termed ''GPinh-5a''; fig. 1a) is a very potent CFTR inhibitor [13, 14]. Here, following a structure–activity study, we identified methylglyoxal-9-propyladenine adducts (fig. 1b), an analogue of 5a named GPact-11a (Grenoble Poitiers CFTR activator-11a), as a selective, water-soluble and nontoxic activator of wt and mutated F508del-CFTR.

MATERIAL AND METHODS

Chemistry

All starting materials were commercially available research-grade chemicals and used without further purification.

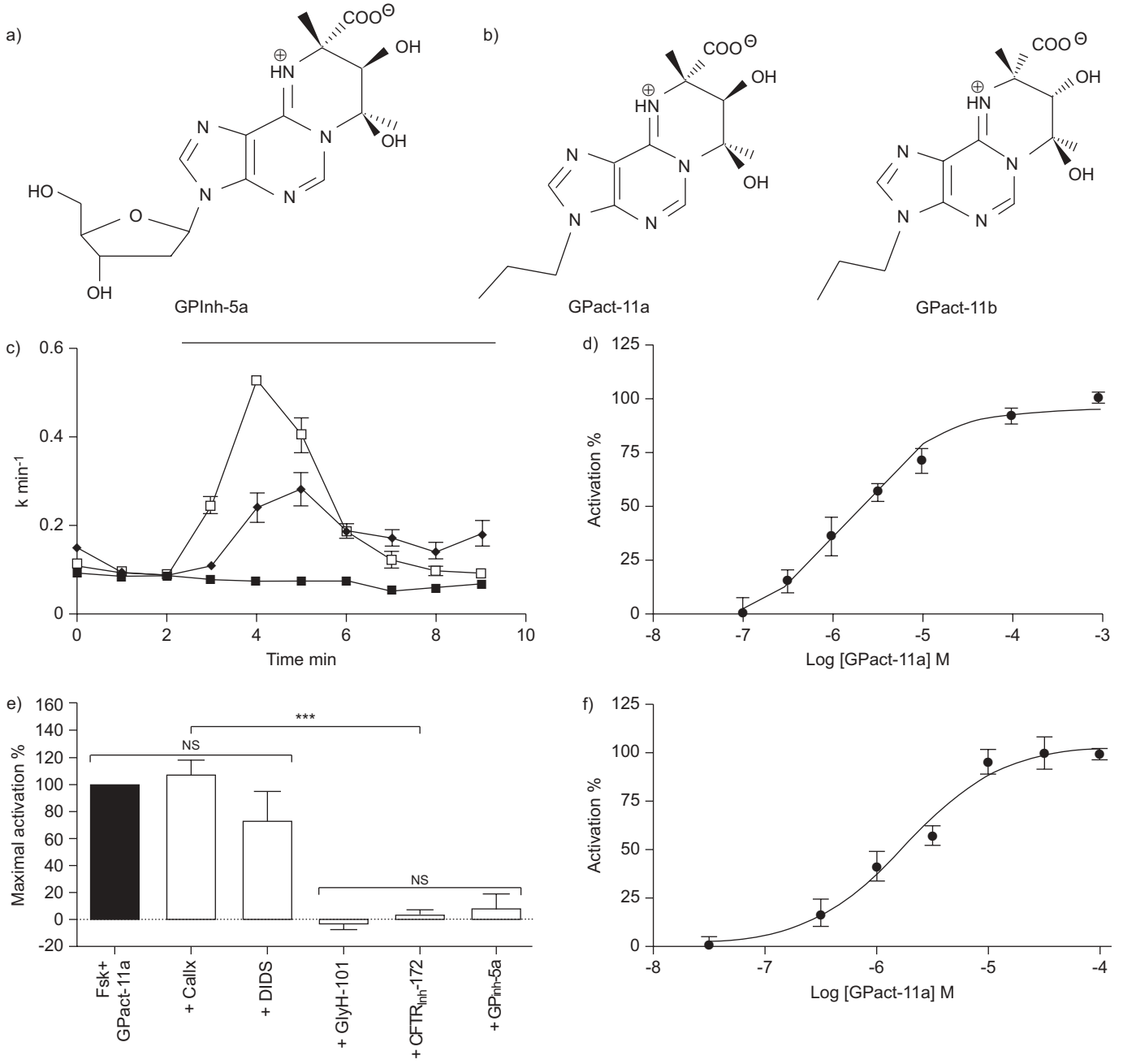

FIGURE 1. a, b) Structural evolution of the methylglyoxal α-aminoazaheterocycle cystic fibrosis transmembrane conductance regulator (CFTR) inhibitor, GPinh-5a (a), to the methylglyoxal-9-propyladenine CFTR activator: GPact-11 (b), a mixture of isomers, the major mixture of enantiomers 11a and the minor one 11b. c) Typical iodide efflux experiments showing potentiation by GPact-11a (100 μM; □) and inhibition by GPinh-5a (1 μM; ■) of the forskolin (Fsk, 1 μM) induced response in wt-CFTR Chinese hamster ovary (CHO) cells (◆: Fsk alone). The horizontal bar above the trace indicated the presence of drugs. d) Concentration–response curves for GPact-11a in presence of Fsk (1 μM) in wt-CFTR CHO cells. e) Effect of GlyH-101 (10 μM), $CFTR_{inh}$-172 (10 μM), GPinh-5a (200 pM), DIDS (4, 4^1-diisothiocyanatostilbene-2, 2^1-disulfonic acid); 100 μM) and calixarene (calix; 100 nM) on Fsk (1 μM) + GPact-11a (100 μM) response. f) Concentration–response curves for GPact-11a in the presence of Fsk (1 μM) in Calu-3 cells. Data are presented as mean±SEM; n=4 for each condition. NS: nonsignificant. ***: $p<0.001$.

Reactions were monitored by analytical thin layer chromatography with fluorescent indicator UV254 from Macherey-Nagel (Duren, Germany). ^{1}H and ^{13}C nuclear magnetic resonance (NMR) spectra were recorded on a Bruker avance (Madison, WI, USA) 400 (400 and 100 MHz). Chemical shifts are reported in ppm relative to the residual signal of the solvent, and the signals are described as singlet (s), broad singlet (bs), doublet (d), triplet (t), doublet of doublet (dd), quartet (q), multiplet (m); coupling constants are reported in Hz. To the commercially available concentrated aqueous solution of methyglyoxal (40%; 1.5 mL, 9.0 mmol), 9-propyladenine (480 mg, 1.8 mmol) and water (5 mL) were added. Argon was flushed through the solution and the mixture was heated at 50°C for 17 h. After evaporation under reduced pressure, the residue was chromatographed on C18 reversed phase (10 g) eluting with H_2O and then H_2O-methanol (MeOH) (95:5) to give GPact-11a (24%) and GPact-11b (17%).

Chemical properties of GPact-11 isomers

GPact-11a. Melting point: 152–154°C; ^{1}H NMR (400 MHz, D_2O): 8.84 (1H, s, CH_{Ar}), 8.20 (1H, s, CH_{Ar}), 4.53 (1H, s, CH), 4.20 (2H, t, J=7.0 Hz, CH_2), 1.87–1.81 (2H, m, CH_2), 1.75 (3H, s, CH_3), 1.67 (3H, s, CH_3), 0.85 (3H, t, J=7.0 Hz, CH_3); ^{13}C NMR (100 MHz, D_2O): 176.6 (COOH), 146.8 (C_{IV}), 145.1 (CH_{Ar}), 142.7 (CH_{Ar}), 117.6 (C_{IV}), 89.2 (C_{IV}), 70.6 (CH), 63.3 (C_{IV}), 46.1 (CH_2), 25.7 (CH_3), 22.8 (CH_2), 22.2 (CH_3), 10.2 (CH_3); LRMS (FAB [+], glycerol): m/z 322 ($[M+H]^+$); elemental analysis calculated for $C_{14}H_{19}N_5O_4$, 1/3 H_2O: C 51.37, H 6.06, N 21.39, found C 51.34, H 5.98, N 21.24.

GPact-11b. mp: 102°C; ^{1}H NMR (400 MHz, D_2O pH=7, phosphate buffer): 8.72 (1H, s, CH), 8.23 (1H, s, CH) 4.21 (3H, m, CH_2 and CH), 1.86 (5H, m, CH_2 and CH_3), 1.74 (3H, s, CH_3), 0.84 (3H, t, J=7.0 Hz, CH_3), ^{13}C NMR (50 MHz, D_2O, pH=7, phosphate buffer) 176.1 (COO), 146.5 (C_{IV}), 144.2 (CH_{Ar}), 144.0 (CH_{Ar}), 117.5 (C_{IV}), 74.1 (CH), 60.7 (C_{IV}), 45.5 (CH_2), 26.0 (CH_3), 24.4 (CH_2), 18,0 (CH_3), 9.6 (CH_3), HRMS (EI) calc. for $C_{14}H_{19}N_5O_4$: $[M+H]^+$ 322.1515, found 322.1507, $[M+Na]^+$ 344.1335, found 344.1343.

Other chemicals

3-[(3-trifluoromethyl)-phenyl]-5-[(4-carboxyphenyl)methylene]-2-thioxo-4-thiazolidinone ($CFTR_{inh}$-172) and *N*-(2-naphthalenyl)-[(3,5-dibromo-2,4-dihydroxyphenyl)methylene]glycine hydrazide (GlyH-101) were from VWR International (Fontenay-sous-Bois, France). GPinh-5a was synthesised as previously described [13]. Miglustat was from Toronto research chemicals (Toronto, ON, Canada). All other chemicals were from SIGMA (St Louis, MO, USA). All chemical agents were dissolved in DMSO, with the exception of GPact-11a, GPinh-5a, amiloride, miglustat and GlyH-101, which were dissolved in H_2O, and isoprenaline, which was dissolved in NaCl 0.9%.

Cell culture

Cell lines were cultured as previously described: Chinese hamster ovary (CHO), Calu-3, JME/CF15 [15], CF-KM4 and MM39 [16], NuLi and CuFi-1 [17] and CFPAC-1 [18]. HEK293 cells were cultured and transiently transfected with the pEGFP-CFTR wt or F508del as already described [19, 20].

Freshly isolated human ciliated epithelial cells

The study was approved by our local institutional ethics committee. Human lung tissues were obtained from seven patients: three non-CF males with a mean age of 61 yrs, a non-CF female aged 65 yrs, a F508del/F508del-CFTR male aged 37 yrs, a F508del/R1066C female aged 26 yrs and a F508del/H1085R-CFTR female aged 23 yrs. Following lobectomy, lung samples, distant from the malignant lesion, were quickly dissected. After removal of connective tissues, cartilage and smooth muscle tissues, epithelial tissues were cut out in small segments. Single epithelial cells were mechanically dissociated by passing the bronchial tissue repeatedly through fire-polished Pasteur pipettes. Dissociated ciliated human epithelial cells were plated onto culture dishes for 6 h in culture medium (Dulbecco's modified Eagle medium /HAM-F12, insulin 5 $\mu g \cdot mL^{-1}$, transferin 7.5 $\mu g \cdot mL^{-1}$, hydrocortisone 10^{-6} M, endothelial cell growth supplement 2 $\mu g \cdot mL^{-1}$, epithelial growth factor 25 $ng \cdot mL^{-1}$, T3 3.10^{-5} M, L-glutamine 200 mM, and penicillin/streptomycin 100 $\mu g \cdot mL^{-1}$).

Animals

Wt (*cftr*$^{+/+}$) and *cftr* knock-out (*cftr*$^{-/-}$) female mice (C57Bl/6 129-CFTRtm1Unc) obtained from CDTA (*Centre de Distribution, Typage et Archivage Animal*, Orléans, France), were studied between the age of 3 and 4 weeks. To prevent lethal intestinal obstruction, mice were fed with movicol® (30 $g \cdot L^{-1}$) in drinking water.

Functional analysis of CFTR activity in vitro

CFTR Cl^- channel activity was assayed by iodide (^{125}I) efflux [21] or by single-cell fluorescence imaging, using the potential-sensitive probe, bis-(1,3-diethylthiobarbituric acid)trimethine oxonol ($DiSBAC_2(3)$; Molecular Probes, Eugene, OR, USA) [22]. Iodide efflux curves were constructed by plotting rate of ^{125}I *versus* time. All comparisons were based on maximal values for the time-dependent rates (k=peak rates, min^{-1}) excluding the points used to establish the baseline (k peak-k basal, min^{-1}). The results of fluorescence imaging are presented as transformed data to obtain the percentage signal variation (Fx) relative to the time of addition of the stimulus, according to the equation: $Fx=((Ft-F0)/F0)\times 100$ where Ft and F0 are the fluorescent values at the time t and at the time of addition of the stimulus, respectively. For histogram representation, the values correspond to the level of stable variation of fluorescence induced by each drug. CFTR Cl^- currents were measured in the broken-patch, whole-cell configuration of the patch-clamp technique [20].

cAMP concentration measurements

The intracellular cAMP was evaluated with the cAMP HTS Immunoassay Kit (Millipore, Billerca, MA, USA) following the manufacturer instructions. Luminescence was measured with TopCount NXT (PerkinElmer, Waltham, MA, USA) microplate reader.

Short-circuit current measurements

The apical membrane Cl^- current was measured on mice colonic epithelium as already described [15] or after a depolarisation protocol [23] using a serosal-to-mucosal gradient with the following bath solution: apical, 107 mM K-gluconate, 4.5 mM KCl, 25 mM $NaHCO_3$,1 mM $MgSO_4$, 1.8 mM Na_2HPO_4, 0.2 mM NaH_2PO_4, 5.75 mM Ca-gluconate, 12 mM D-glucose; basolateral, 111.5 mM KCl, 25 mM $NaHCO_3$, 1 mM

$MgSO_4$, 1.8 mM Na_2HPO_4, 0.2 mM NaH_2PO_4, 1.25 mM $CaCl_2$, 12 mM D-glucose [23].

Salivary secretion assay

The salivary secretion was collected in response to subcutaneous injection of different pharmacological agents as described [24, 25]. Basal salivary secretion due to cholinergic response was inhibited by atropine (1 mM).

Data analysis

Data are presented as mean±SEM, where n refers to the number of isolated cell (single cell measurements), cell populations (iodide efflux and cAMP measurements) and N to the number of animals. Datasets were compared with an unpaired t-test. All graphs were plotted with GraphPad Prism 5.0 for Windows (GraphPad Software, San Diego, CA, USA). A p-value <0.05 were considered as statistically significant.

RESULTS

Effect of GPact-11a on wt-CFTR activity

We first examined the effect of GPact-11a on CHO cells stably expressing wt-CFTR with our robotic cell-based primary screening assay using iodide efflux measurement. This assay allows a rapid detection of CFTR channel activation or inhibition. The adenylate cyclase activator Fsk (fig. 1c) stimulated an iodide efflux in wt-CFTR CHO cells (relative rate=k_{peak}-k_{basal}=0.44±0.01 min^{-1}, n=4; fig. 1c). This efflux was inhibited by GPinh-5a (fig. 1c). In the experiment presented in figure 1c, GPact-11a potentiated the Fsk-induced response to a relative rate of 0.38±0.02 min^{-1} (n=4). The stimulation of CFTR by GPact-11a, in the presence of Fsk followed a dose-dependent relationship described by a half-maximal effective concentration (EC_{50}) of 2.1±1.3 μM (n=4; fig. 1d). Similar experiments were performed with the minor isomer GPact-11b leading to an EC_{50} of 2.9±0.9 μM (data not shown, n=4). The effect of GPact-11a was fully inhibited by $CFTR_{inh}$-172, GlyH-101 and GPinh-5a, three selective CFTR inhibitors [13, 26, 27] but was not affected by DIDS and calixarene, two non-CFTR inhibitors [28] (fig. 1e). We extended our study to evaluate the effect of GPact-11a on endogenous wt-CFTR in the human pulmonary epithelial cell line Calu-3, and found an EC_{50} of 1.8±1.3 μM in presence of Fsk (fig. 1f).

GPact-11a is an activator of wt-CFTR chloride channels

We then explored the cellular cAMP level in wt-CFTR CHO in response to several concentrations of GPact-11a. Figure 2a shows that GPact-11a has no effect on the basal cellular cAMP level. However, because we measured a low level of cAMP with Fsk, we wished to confirm these results in a human tracheal airway epithelial cell line (MM39) endogenously expressing wt-CFTR. Figure 2b shows the strong increase of cAMP level stimulated by Fsk but confirmed that GPact-11a had no effect on cAMP signalling pathway.

We compared the effect of GPact-11a on CFTR activity, in the presence or absence of Fsk, using single-cell fluorescence imaging technique applied to MM39. As expected, we observed that Fsk increased the recorded fluorescence signal. The signal was then further increased by GPact-11a and fully inhibited by $CFTR_{inh}$-172 (fig. 3a). Interestingly, as shown figure 3b, GPact-11a increased the recorded fluorescence signal in the absence of Fsk and this effect was inhibited by $CFTR_{inh}$-172. Figure 3c summarises the result obtained by a stimulation of Fsk or GPact-11a compared with the amplitude of the response generated by the co-application of GPact-11a+Fsk. These results demonstrated an additive and not a synergic effect suggesting two different mechanisms of action for Fsk and GPact-11a. We determined the concentration-response effect of GPact-11a, in the presence or absence of Fsk, and calculated an EC_{50} of 2.8±0.1 μM and 2.1±0.1 μM, respectively (fig. 3d). We determined the effect of GPact-11a on human ciliated epithelial cells freshly dissociated from lung samples (freshly isolated HBE; fig. 3f). In these cells, GPact-11a induced a strong increase of the fluorescence inhibited by $CFTR_{inh}$-172 (fig. 3e). Finally, GPact-11a activated wt-CFTR on HEK293 cells transiently expressing EGFP-wt-CFTR proteins, in tracheal (MM39) and bronchial (NuLi) cell lines and in freshly isolated HBE cells (fig. 3f). Importantly, the CFTR response in HBE was 6-fold higher than in cell lines.

We used whole-cell patch-clamp technique to record CFTR currents on HEK293 cells transiently expressing EGFP-wt-CFTR proteins. After stimulation with GPact-11a, the whole-cell current increased linearly and reversed at -40 mV (fig. 4a and b) confirming its Cl^- nature. This Cl^- current was inhibited by the extracellular perfusion of $CFTR_{inh}$-172 (fig. 4).

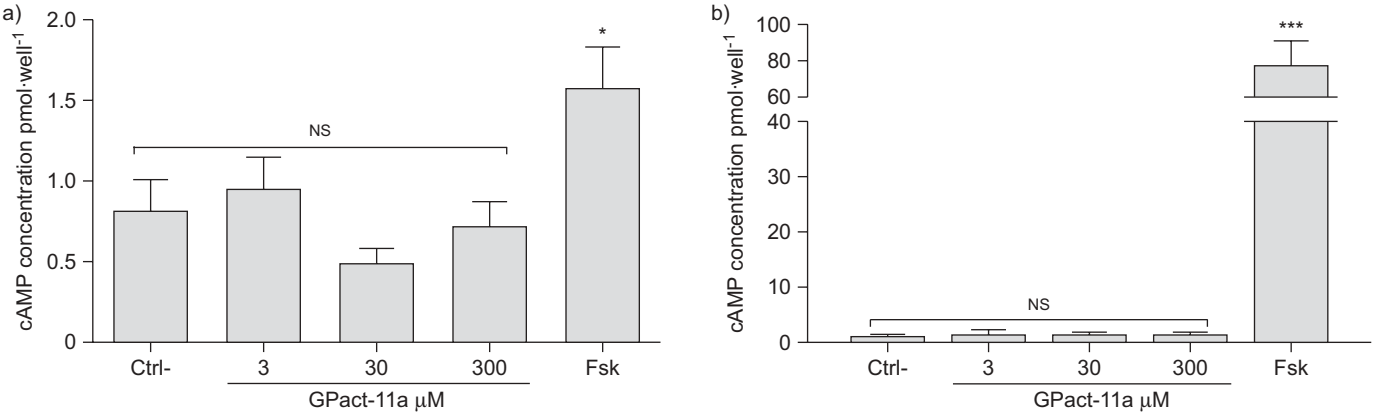

FIGURE 2. Effect of GPact-11a on cAMP level in wt-cystic fibrosis transmembrane conductance regulator a) Chinese hamster ovary (CHO) and b) MM39 cell lines. Forskolin (Fsk; 10 μM) was used as positive control. Ctrl-: untreated cells. n=6 for wt-CFTR CHO cells and n=12 for MM39 cells. NS: nonsignificant. *: $p<0.05$; ***: $p<0.001$.

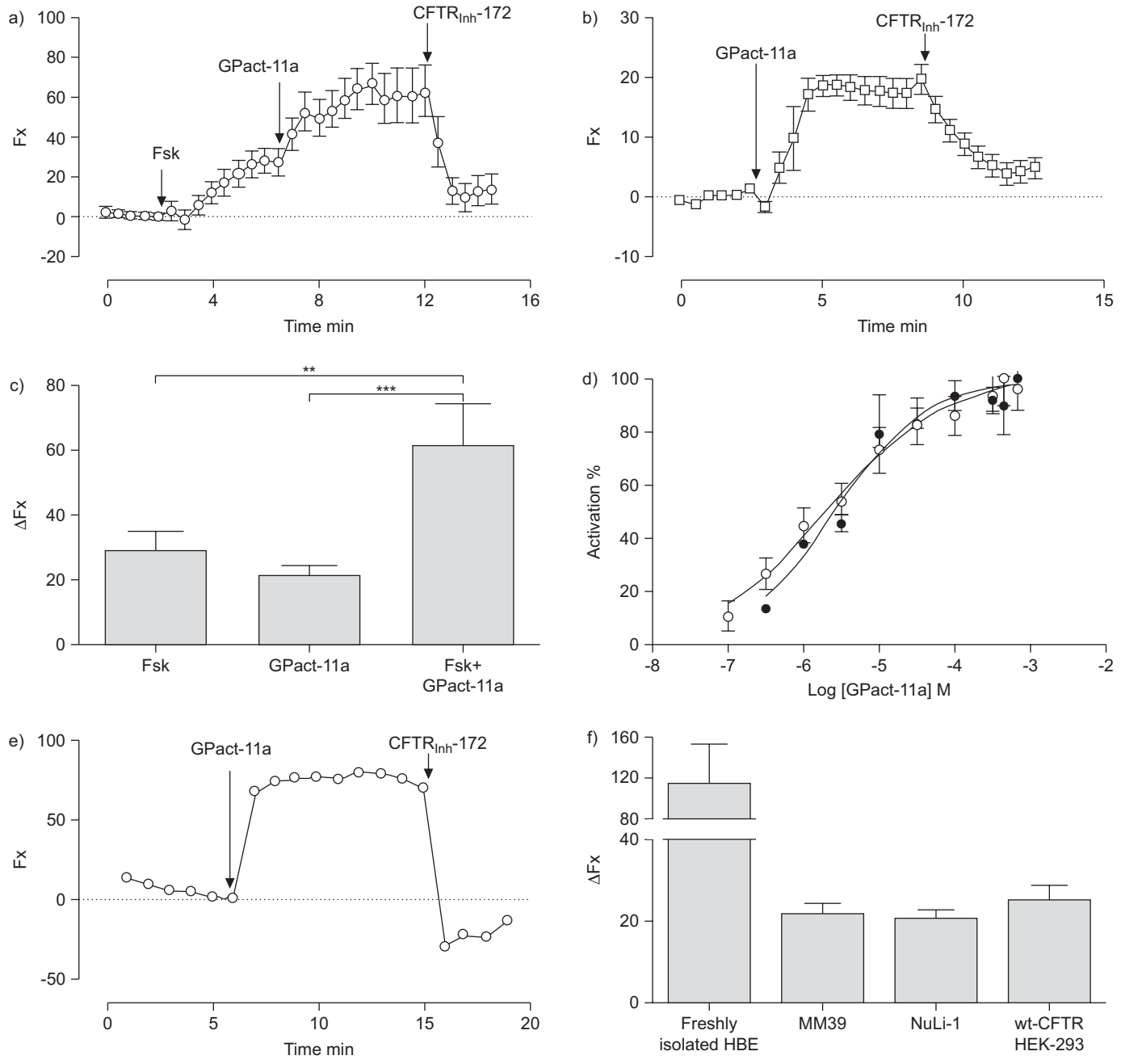

FIGURE 3. Functional evaluation of GPact-11a on wt-cystic fibrosis transmembrane conductance regulator (CFTR) by bis-(1,3-diethylthiobarbituric acid)trimethine oxonol assay. a, b) Time courses of relative fluorescence (Fx) showing the effect of forskolin (Fsk), GPact-11a and $CFTR_{inh}$-172 on MM39 cells. c) Histograms showing the additional effect of Fsk and GPact-11a on MM39 cells. n=12 for each condition in a–c. d) Concentration–response curves of GPact-11a in MM39 cells in presence (○) or absence (●) of Fsk (1 μM). Data point reports the normalisation of the relative fluorescence collected from separate experiments with a total of 30 cells. e) Time course of Fx showing the effect of GPact-11a on freshly dissociated human bronchial ciliated epithelial cells (HBE cells). f) Histograms summarising the effect of GPact-11a obtained on HEK293 cells transiently expressing EGFP-wt-CFTR proteins (n=52), in MM39 (n=83) and NuLi (n=12) cell lines and in freshly isolated HBE cells (n=14 obtained from four patients). Concentrations were Fsk 1 μM, GPact-11a 300 μM (except for d) and $CFTR_{inh}$-172 10 μM.

GPact-11a is an activator of rescued F508del-CFTR chloride channels

We determined by single-cell fluorescence imaging, the effect of GPact-11a on human CF tracheal glandular epithelial cells endogenously expressing F508del-CFTR (CF-KM4 cells). The defective trafficking characteristic of F508del-CFTR can be corrected by miglustat [22, 29]. A sharp increase of fluorescence, inhibited by $CFTR_{inh}$-172 (fig. 5a) or GlyH-101 (data not shown), was recorded after addition of GPact-11a on miglustat-corrected CF-KM4 cells. On the contrary, GPact-11a had no effect on untreated CF-KM4 cells (fig. 5a), confirming the CFTR selectivity of GPact-11a. On miglustat-corrected CF-KM4 cells, GPact-11a induced a concentration-dependent elevation of fluorescence with an EC_{50} of 34.3±1.8 μM

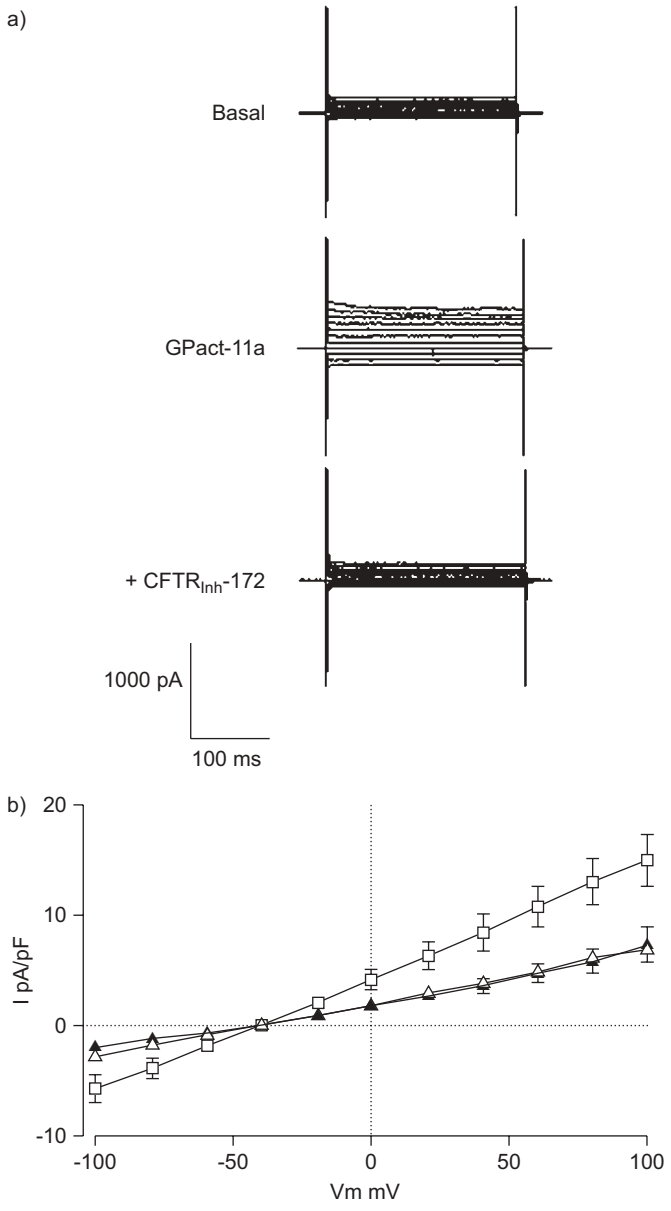

FIGURE 4. Patch clamp experiments on HEK293 cells transfected with wt-CFTR. a) Representative traces of whole cell Cl^- currents elicited from a holding potential of -40 mV to a series test potentials from -100 to 100 mV in 20 mV increments. b) Corresponding current (I)–voltage (Vm) relationships normalised by cell capacitance: basal (▲; n=7); GPact-11a (□; 300 μM, n=7); GPact-11a+$CFTR_{inh}$-172 (△; 10 μM, n=7).

(fig. 5b). Complementary studies performed on several human epithelial cell lines endogenously or transiently expressing F508del-CFTR are presented in figure 5c. Again, following the rescue of F508del-CFTR to the plasma membrane by miglustat, GPact-11a activated F508del-CFTR on HEK293 cells transiently expressing EGFP-F508del-CFTR proteins and in nasal (CF15), tracheal (CF-KM4), bronchial (CuFi) and pancreatic (CFPAC) CF cell lines (fig. 5c). Finally, we evaluated the effect of GPact-11a on ciliated epithelial cells freshly dissociated from human lungs of different CF genotype. The mutation R1066C is a missense mutation in the second transmembrane domain of CFTR [30] and causes a severe CF phenotype. R1066C-CFTR protein is not correctly processed and, unlike F508del-CFTR, this defect can not be corrected in reduced temperature or butyrate-treated cells [31]. The mutation H1085R is a severe and rare missense mutation identified by MERCIER *et al.* [32]. H1085R-CFTR protein presents a trafficking defect which can be corrected by F508del-CFTR corrector [33]. Figure 5d shows that in miglustat-pretreated cells from 3 CF patients with different genotypes, GPact-11a induced a strong increase of the fluorescence.

Whole-cell patch-clamp currents were recorded in HEK293 cells transiently expressing EGFP-F508del-CFTR proteins (fig. 6). Whereas GPact-11a has no effect in these cells cultured at 37°C (left traces; fig. 6a and b), a linear non-voltage-dependent Cl^- current was recorded for cells treated by miglustat (middle traces; fig. 6a and b) or cultured at low temperature (right traces; fig. 6a and b). F508del-CFTR Cl^- currents activated by GPact-11a were inhibited by $CFTR_{inh}$-172 (fig. 6a and b).

Ex vivo *evaluation of GPact-11a*

We determined the effect of GPact-11a on the transepithelial ion transport under short-circuit current (I_{sc}) conditions on *cftr*$^{+/+}$ and *cftr*$^{-/-}$ mice colonic epithelium. In these conditions, *cftr*$^{+/+}$ tissues had a mean transepithelial resistance (R_{te}) of $40.1 \pm 1.5\ \Omega \cdot cm^2$ and a mean spontaneous I_{sc} of $42.1 \pm 2.7\ \mu A \cdot cm^{-2}$ (n=88). For *cftr*$^{-/-}$ tissues, R_{te} and I_{sc} were $34.4 \pm 2.5\ \Omega \cdot cm^2$ and $-2.7 \pm 2.9\ \mu A \cdot cm^{-2}$ (n=24), respectively. All experiments were conducted in presence of 100 μM amiloride to inhibit the resting Na^+ current set by the activity of the epithelial sodium (ENaC) channel. The contribution of the transepithelial Cl^- transport (I_{Cl}) was investigated after depolarisation of the basolateral membrane with a solution containing high potassium concentration [23]. This procedure allowed measurement of changes in the apical anion conductance, avoiding contamination in the current response from, for instance, charybdotoxin-sensitive apical K^+ channels [23]. Following depolarisation, the average R_{te} and I_{sc} in *cftr*$^{+/+}$ colon were $40.2 \pm 1.4\ \Omega \cdot cm^2$ and $147 \pm 7\ \mu A \cdot cm^{-2}$ (n=12), respectively. Adding increasing concentrations of GPact-11a to both sides of *cftr*$^{+/+}$ colonic epithelium induced a dose-dependent elevation of I_{sc} with an EC_{50} of 175.6 ± 1.1 μM (n=3; fig. 7a and c). It was inhibited by glibenclamide (fig. 7a). On the contrary, application in the same experimental conditions of GPact-11a had no effect on *cftr*$^{-/-}$ colonic epithelium (fig. 7b). Addition of glucose increased I_{sc} showing the viability of the tissues (fig. 7b).

Further experiments were carried out without the depolarisation protocol to determine the specificity of GPact-11a. Firstly, we permeabilised either apical or basolateral membrane with $200\ \mu g \cdot mL^{-1}$ of nystatin for 30 min and then measured I_{sc}. As shown in figure 7d, permeabilising the apical membrane with nystatin prevented the GPact-11a effect (n=5) whereas basolateral permeabilisation had no significant effect on GPact-11a I_{sc} response (n=4). Secondly, in *cftr*$^{+/+}$ colonic epithelium, the elevation of I_{sc} by GPact-11a was inhibited by $CFTR_{inh}$-172 and glibenclamide but not affected by DIDS (fig. 7e). Finally, we found, with this protocol, no effect of GPact-11a on *cftr*$^{-/-}$ colonic epithelium (n=4, data not shown).

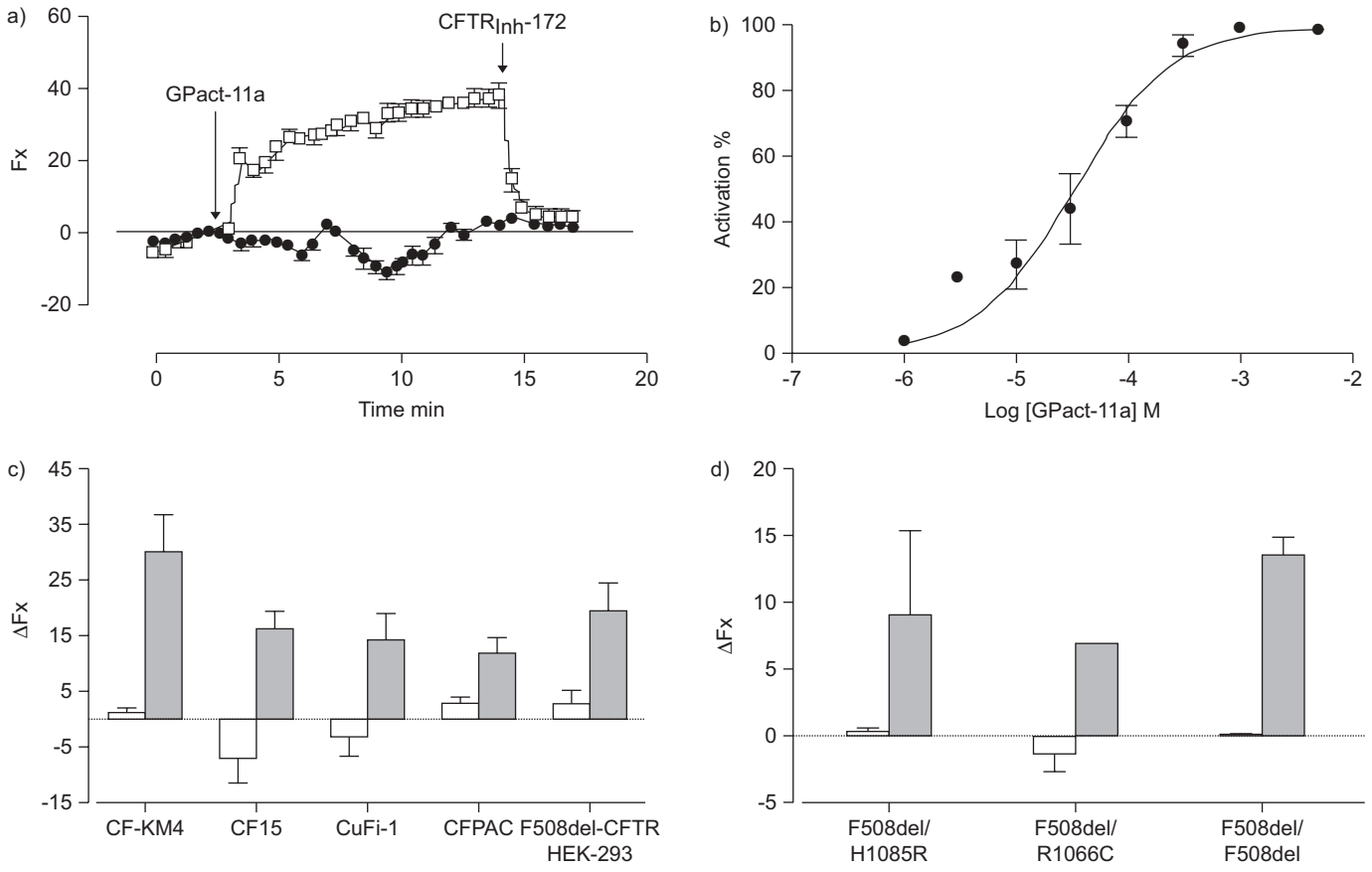

FIGURE 5. Functional evaluation of GPact-11a on F508del-cystic fibrosis transmembrane conductance regulator (CFTR) by bis-(1,3-diethylthiobarbituric acid)trimethine oxonol assay. a) Time courses of relative fluorescence (Fx) showing the effect of GPact-11a and $CFTR_{inh}$-172 on untreated CF-KM4 cells (●) or on CF-KM4 cells corrected by miglustat (□). n=12 for each condition. b) Concentration–response curve of GPact-11a on CF-KM4 cells previously corrected by miglustat. Data points report the normalisation of the relative fluorescence collected from three separate experiments with a total of 30 cells. c) Effect of GPact-11a on F508del-CFTR cell lines untreated (□) or corrected (■) by miglustat ($8<n<127$). d) Effect of GPact-11a on human bronchial ciliated epithelial cells cells freshly isolated from lungs with different cystic fibrosis genotypes (F508del/F508del-CFTR (n=4), F508del/R1066C (n=7) and F508del/H1085R-CFTR (n=9)). Concentrations were $CFTR_{inh}$-172 10 μM and GPact-11a 300 μM (except for b). Cells were cultured with miglustat 100 μM for 2 h (except for CFPAC: 100 μM, 24 h).

In vivo *evaluation of GPact-11a*

To evaluate the *in vivo* effect of GPact-11a on $cftr^{+/+}$ and $cftr^{-/-}$ mice, we used a noninvasive measurement technique of salivary secretion [25]. First, we determined the secretory capacity of salivary secretion in $cftr^{+/+}$ mice by stimulating the salivary gland with GPact-11a alone. GPact-11a by itself did not elevate salivary secretion (n=3; fig. 8a). On the contrary, isoprenaline stimulated salivary secretion with a mean of 36.9 ± 5.2 $\mu g \cdot min^{-1} \cdot g^{-1}$ (n=19; fig. 8a). GPact-11a potentiated isoprenaline-induced secretion (70.2 ± 9.0 $\mu g \cdot min^{-1} \cdot g^{-1}$, n=7; fig. 8a). Figure 8b summarises the results obtained with increasing concentrations of GPact-11a and showed that GPact-11a, in the presence of isoprenaline, induced a dose-dependent salivary secretion in $cftr^{+/+}$ mice with an EC_{50} of 7.1 ± 1.1 μM ($5<n<8$; fig. 8c). The isoprenaline/GPact-11a-induced salivary secretion was inhibited by GPinh-5a and GlyH-101 (fig. 8d and e). Finally, we found no effect of isoprenaline and GPact-11a on the salivary secretion of $cftr^{-/-}$ mice (fig. 8f).

DISCUSSION

In the present study, we report on the discovery of methylglyoxal-9-propyladenine adducts named GPact-11a, as a selective, water-soluble and nontoxic activator of wt and F508del-CFTR. The most important results of our present investigation are: 1) GPact-11a is a novel activator of CFTR chloride channels in human airway epithelial cell lines; 2) GPact-11a activates rescued F508del-CFTR in nasal, tracheal, bronchial and pancreatic human CF epithelial cells; 3) GPact-11a is an activator of wt-CFTR and rescued F508del-CFTR in human ciliated epithelial cells freshly dissociated from CF and non-CF lung samples; 4) *ex vivo*, GPact-11a stimulates colonic chloride secretion in $cftr^{+/+}$ mice; 5) *in vivo*, it increases salivary secretion in $cftr^{+/+}$ mice; 6) GPact-11a is selective for CFTR because, in all our experimental conditions, we inhibited the effect of GPact-11a by the established CFTR inhibitors $CFTR_{inh}$-172, GlyH-101, glibenclamide or GPinh-5a. In addition, we did not observe activation of any non-CFTR channels in uncorrected F508del-CFTR cells and on $cftr^{-/-}$ mice.

Structural determinants for CFTR activation

In the chemical structure of GPact-11a (fig. 1b), three main elements can be distinguished: 1) the purine aromatic heterocycles composed of fused pyrimidine and imidazole rings;

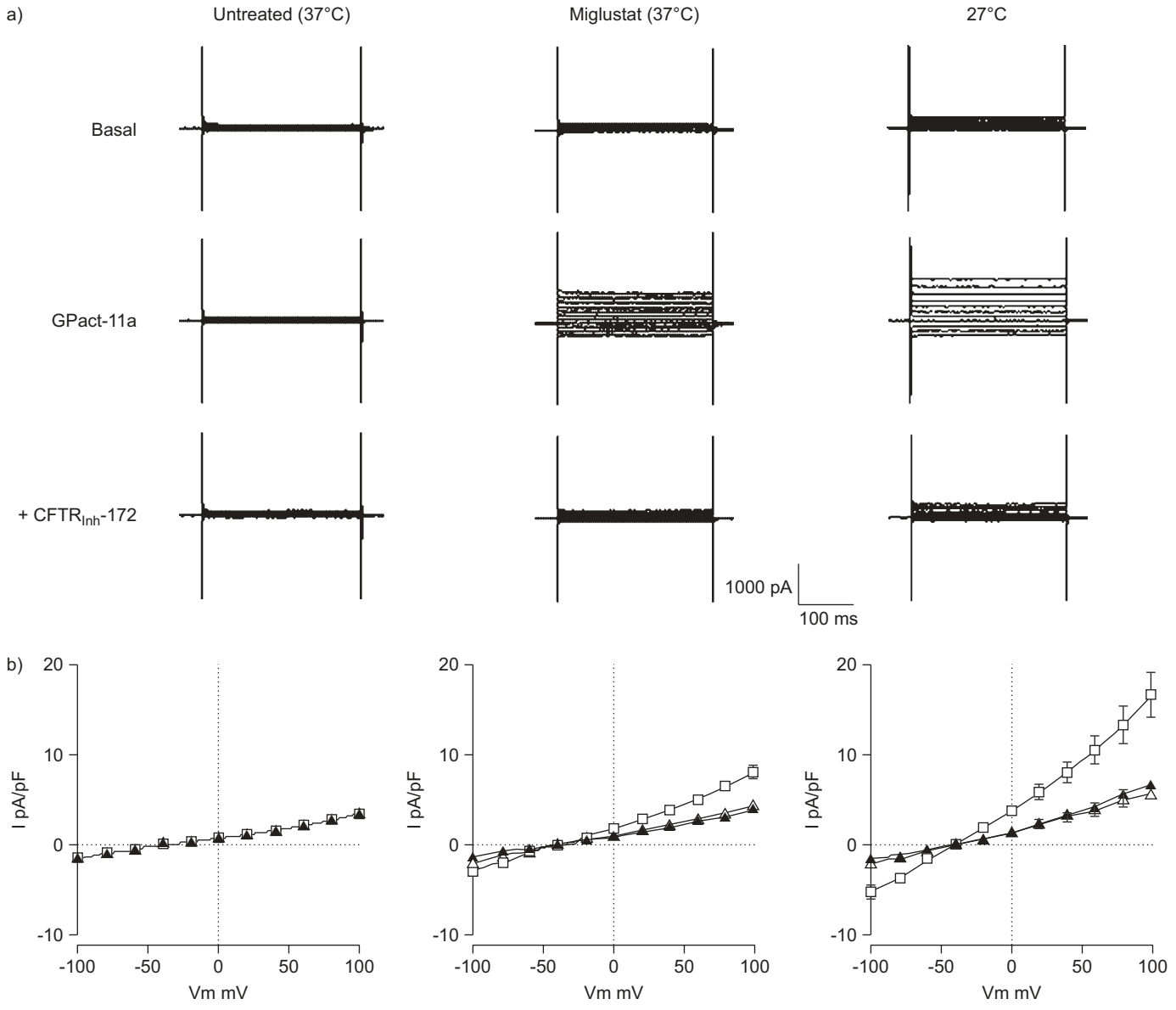

FIGURE 6. Whole-cell patch clamp recordings with F508del-cystic fibrosis transmembrane conductance regulator (CFTR) HEK293 cells untreated (n=5), corrected by miglustat (100 μM; 4 h, n=5) or cultured at 27°C (24 h, n=5) a) Representative traces of whole-cell Cl^- currents elicited from -100 to 100 mV, in 20 mV steps. b) Corresponding current(I)–voltage (Vm) relationships normalised by cell capacitance. Concentrations were GPact-11a 300 μM and $CFTR_{inh}$-172 10 μM. ▲: basal; □: GPact-11a; △: +$CFTR_{inh}$-172.

2) a hydrophobic propyl side chain attached to a nitrogen atom of the purine; and 3) the hydrophilic rings formed by condensation of methylglyoxal with 9-propyladenine. This latter ring probably includes the main pharmacophore because 9-propyladenine is not active on the CFTR channel (data not shown). The structure of the activator GPact-11a is close to the structure of the inhibitor GPinh-5a. In both structures, the first and third elements are present. This observation suggests a potential common binding site on the target involving the hydrophilic pharmacophore (*i.e.* the third element). The 9-propyl hydrophobic substituent in GPact-11a is replaced by a 9-(2-deoxyribos-1-yl) substituent which is hydrophilic in GPinh-5a. This substitution produces a shift from an activator to an inhibitor. GPinh-5a and GPact-11a are both zwitterionic at physiological pH, carrying a carboxylate function and a protonated imino group, two properties explaining their high water solubility.

In comparison with the activators previously described, some similarities can be mentioned. The xanthines activators are purine heterocycles substituted with hydrophobic substituents attached to a nitrogen atom on the purine (methyl, cyclohexyl, cyclopentadienyl, isopropyl) [6]. Hydrophobic substituents attached to a nitrogen atom also are present in pyrrolo [2,3-b]pyrazines (butyl in RP107 and RP108) [15] and in the benzimidazolones activators (ethyl in 1-EBIO and DCEBIO) [6]. These activators are made of two fused 6-member and 5-member rings like the purine heterocycle in GPact-11a. Some benzoquinolizinium activators also present a hydrophobic side

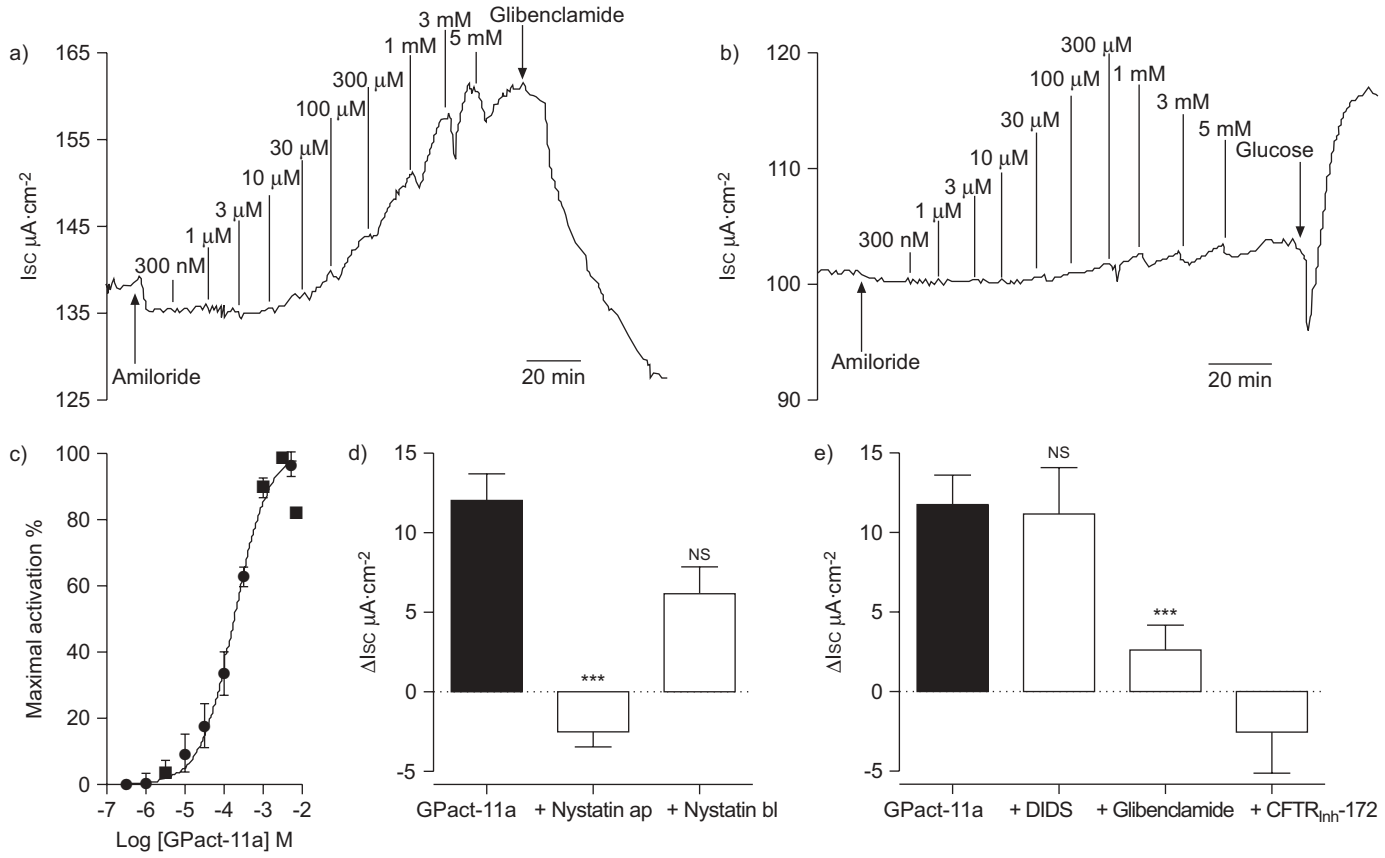

FIGURE 7. Ussing chambers recordings of short-circuit current (I_{sc}) in mice ascending colon. a) Typical example of the effect of increasing concentrations of GPact-11a added on both sides on *cftr*$^{+/+}$ mice colon. Amiloride (100 µM added on mucosal side) was used to inhibit residual epithelial sodium activity and glibenclamide (500 µM added on both sides) was used to inhibit cystic fibrosis transmembrane conductance regulator (CFTR). b) Typical example showing the effect of increasing concentration of GPact-11a added on both sides on *cftr*$^{-/-}$ mice colon. Glucose (40mM added on both sides) was used to verify the reactivity of the tissues. The trace is representative of three separate experiments. c) Dose–response curve of GPact-11a effect on *cftr*$^{+/+}$ mice colon (n=3). d) GPact-11a-induced I_{sc} after permeabilisation by nystatin (200 µg·mL^{-1}, 30 min) added on the apical (ap, n=5) or basolateral (bl, n=4) membrane. e) Effect of DIDS (4, 4^{1}-diisothiocyanatostilbene-2, 2^{1}-disulfonic acid); 500 µM, n=4), glibenclamide (500 µM, n=18) and $CFTR_{inh}$-172 (100 µM, n=5) on GPact-11a-induced I_{sc}. DIDS was pre-incubated 10 min before the experiment. NS: nonsignificant. ***: $p<0.001$.

chain, butyl in MPB-91 and MPB-104, linked to an aromatic heterocycle composed of three fused 6-member rings [6].

Towards a new generation of CFTR activators

Compared with other ion channels, such as voltage-dependent channels or neurotransmitter-activated channels [34–36], CFTR pharmacology is still in its infancy. No selective ligands, activators or inhibitors have been approved for clinical use. The CFTR modulators of the first generation were originally identified after investigations of the intracellular signalling pathways. For example, CFTR can be activated by agents that elevate cellular cAMP or stabilise phosphorylated CFTR (phosphatase inhibitors) [6]. However, two receptor signalling pathways (β_2-adrenergic receptors and A_{2B}-adenosine receptors) efficiently activate wt-CFTR by stimulating adenyl cyclase and raising cellular cAMP [9, 11, 37, 38], but fail to activate F508del-CFTR in human airway epithelial cells. In recent years, a series of compounds that show activity *in vitro* has been described. CFTR openers include flavonoids, xanthines [39, 40], benzoquinoliziniums [6] or fluorescein derivatives [41]. However some of these compounds lack selectivity and have low affinity. CFTR activation requires elevation of cAMP and the consequent phosphorylation at the regulatory domain (R domain) by protein kinase A [6, 34]. CFTR activators can act directly on CFTR protein, or indirectly by inhibiting phosphodiesterases (thus elevating cAMP) or inhibiting phosphatases (thus increasing CFTR phosphorylation) [6, 34]. Indirect effects are not expected to be useful for CF pharmacotherapy, as the basic defect is intrinsic to the CFTR protein and not to upstream regulatory pathways. In this study, we identified GPact-11a as a selective and cAMP-independent activator of wt and rescued F508del-CFTR. Therefore, while the mechanism of action of GPact-11a remains unknown, GPact-11a represents an interesting and potential candidate for the development of a future pharmacological therapy in CF because of its water solubility and absence of toxicity.

A corrector plus an activator for a CF bi-therapy?

F508del-CFTR activators are not expected to be effective unless they are associated with a corrector of F508del mistrafficking. Although a single compound with both types of activity is preferable, a bi-therapy involving a corrector plus an activator

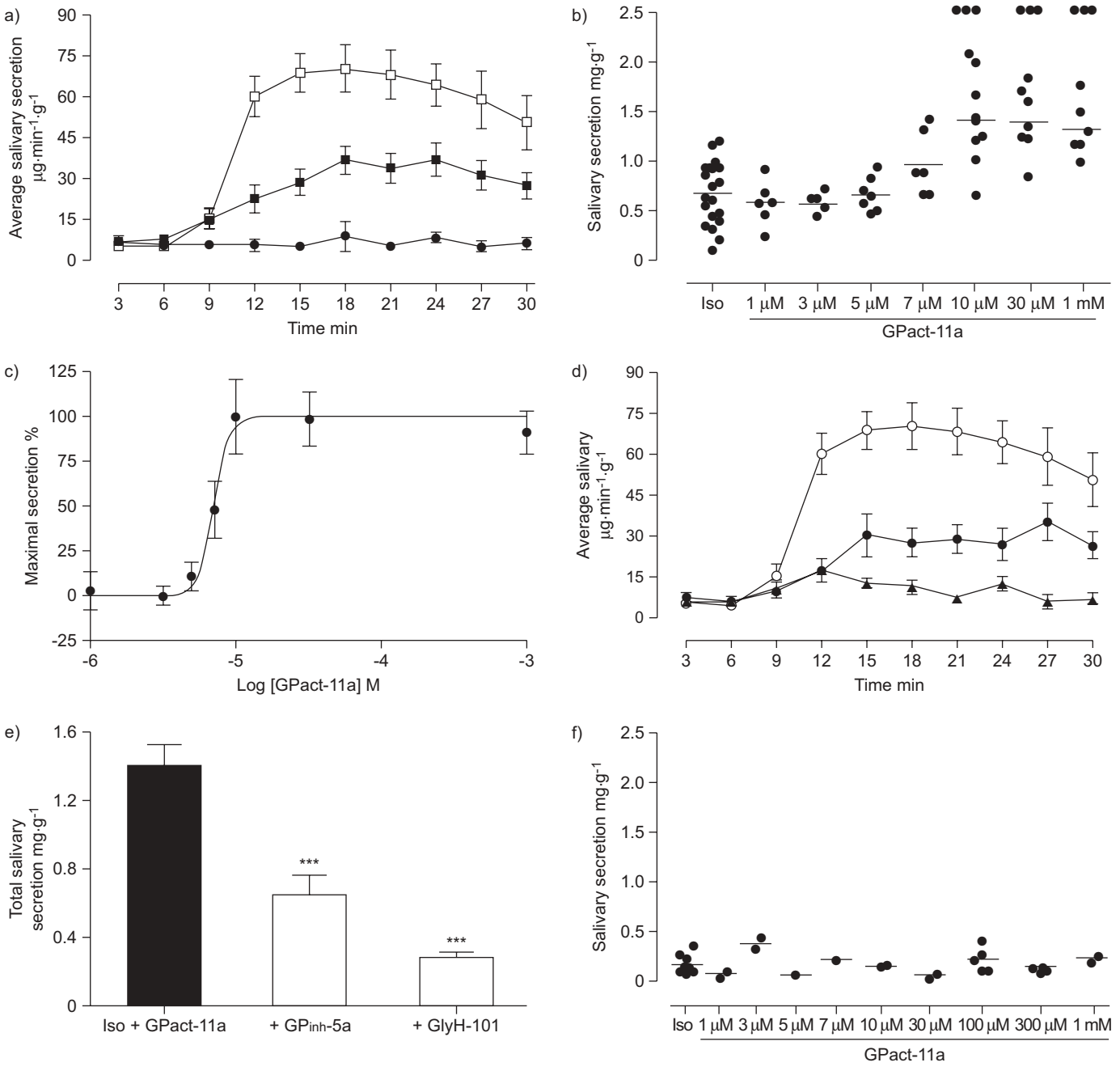

FIGURE 8. *In vivo* evaluation of GPact-11a. a) Average salivary secretion from *cftr*$^{+/+}$ mice induced by GPact-11a (●; 30 µM, n=3), GPact-11a (30 µM) with isoprenaline (10 µM, n=7) (□) or isoprenaline only (■; 10 µM, n=19). b) Total salivary secretion from *cftr*$^{+/+}$ induced by isoprenaline (Iso; 10 µM), with or without increasing concentrations of GPact-11a. c) Corresponding dose–response curve of GPact-11a. d) Average salivary secretion and e) total salivary secretion from *cftr*$^{+/+}$ mice induced by GPact-11a (30 µM) with isoprenaline (10 µM, n=7) (○) and inhibited by two CFTR inhibitors: GPinh-5a (●; 20 pM, n=11) and GlyH-101 (▲; 10 µM, n=4). f) Total salivary secretion from *cftr*$^{-/-}$ induced by isoprenaline (Iso; 10 µM), with or without increasing concentrations of GPact-11a.

could be considered. We believe that the activator GPact-11a is one such valuable candidate. The water-solubility and apparent absence of toxicity of GPact-11a make this agent very attractive. Although a complete pre-clinical safety study will be required, in our preliminary *in vivo* experiments we did not observe serious adverse effects or mortality of mice. The selectivity of a pharmacological agent is a prerequisite before a further industrial and/or clinical development. GPact-11a seems to be selective for CFTR in epithelial cells because we did not observe activation of any types of ionic channels in uncorrected F508del-CFTR cells and in the colon of *cftr*$^{-/-}$ mice. Furthermore, in our models with a functional CFTR, the effect of GPact-11a was systematically inhibited by well-established CFTR inhibitors.

In summary, activation of surface F508del-CFTR will require combinational therapies including agents tailored for rescuing

F508del-CFTR processing, coupled to strategies restoring F508del-CFTR function/regulation at the plasma membrane. Such bi-therapy could include, for example, miglustat with GPact-11a and will be considered in our future studies as a potential therapeutic in CF.

SUPPORT STATEMENT

J. Bertrand was supported by a studentship from Mucovie. B. Boucherle and A. Billet were supported by studentships from Vaincre la mucoviscidose (VLM) and the French ministry of Research, respectively. L. Dannhoffer was supported by a postdoctoral fellowship from VLM and P. Melin-Heschel by a grant from VLM.

STATEMENT OF INTEREST

None declared.

ACKNOWLEDGEMENTS

The authors would like to thank G. Cabrini, J. Glokner-Pagel and M. Merten for providing NuLi and CuFi-1, CFPAC, and MM39 and CF-KM4 cell lines, respectively. We thank P. Corbi and P. Bonnette for access to non-cystic fibrosis and cystic fibrosis human lung samples, respectively.

REFERENCES

1 Anderson MP, Berger HA, Rich DP, *et al.* Nucleoside triphosphates are required to open the CFTR chloride channel. *Cell* 1991; 67: 775–784.
2 Gray MA, Plant S, Argent BE. cAMP-regulated whole cell chloride currents in pancreatic duct cells. *Am J Physiol* 1993; 264: C591–C602.
3 Ratjen F, Doring G. Cystic fibrosis. *Lancet* 2003; 361: 681–689.
4 Sheppard DN, Welsh MJ. Structure and function of the CFTR chloride channel. *Physiol Rev* 1999; 79: Suppl. 1, S23–S45.
5 Dalemans W, Barbry P, Champigny G, *et al.* Altered chloride ion channel kinetics associated with the delta F508 cystic fibrosis mutation. *Nature* 1991; 354: 526–528.
6 Becq F. On the discovery and development of CFTR chloride channel activators. *Curr Pharm Des* 2006; 12: 471–484.
7 Verkman AS, Galietta LJ. Chloride channels as drug targets. *Nat Rev Drug Discov* 2009; 8: 153–171.
8 Bebok Z, Collawn JF, Wakefield J, *et al.* Failure of cAMP agonists to activate rescued deltaF508 CFTR in CFBE41o- airway epithelial monolayers. *J Physiol* 2005; 569: 601–615.
9 Yang H, Shelat AA, Guy RK, *et al.* Nanomolar affinity small molecule correctors of defective Delta F508-CFTR chloride channel gating. *J Biol Chem* 2003; 278: 35079–35085.
10 Olesen SP, Munch E, Moldt P, *et al.* Selective activation of Ca(2+)-dependent K+ channels by novel benzimidazolone. *Eur J Pharmacol* 1994; 251: 53–59.
11 Hwang TC, Wang F, Yang IC, *et al.* Genistein potentiates wild-type and delta F508-CFTR channel activity. *Am J Physiol* 1997; 273: C988–C998.
12 Wang F, Zeltwanger S, Hu S, *et al.* Deletion of phenylalanine 508 causes attenuated phosphorylation-dependent activation of CFTR chloride channels. *J Physiol* 2000; 524: 637–648.
13 Routaboul C, Norez C, Melin P, *et al.* Discovery of alpha-aminoazaheterocycle-methylglyoxal adducts as a new class of high-affinity inhibitors of cystic fibrosis transmembrane conductance regulator chloride channels. *J Pharmacol Exp Ther* 2007; 322: 1023–1035.
14 Routaboul C, Dumas L, Gautier-Luneau I, *et al.* New stereoselective reaction of methylglyoxal with 2-aminopyridine and adenine derivatives: formation of imino acid-nucleic base derivatives in water under mild conditions. *Chem Commun (Camb)* 2002; 10: 1114–1115.
15 Noel S, Faveau C, Norez C, *et al.* Discovery of pyrrolo[2,3-b] pyrazines derivatives as submicromolar affinity activators of wild type, G551D, and F508del cystic fibrosis transmembrane conductance regulator chloride channels. *J Pharmacol Exp Ther* 2006; 319: 349–359.
16 Antigny F, Norez C, Becq F, *et al.* Calcium homeostasis is abnormal in cystic fibrosis airway epithelial cells but is normalized after rescue of F508del-CFTR. *Cell Calcium* 2008; 43: 175–183.
17 Dechecchi MC, Nicolis E, Norez C, *et al.* Anti-inflammatory effect of miglustat in bronchial epithelial cells. *J Cyst Fibros* 2008; 7: 555–565.
18 Lipecka J, Norez C, Bensalem N, *et al.* Rescue of DeltaF508-CFTR (cystic fibrosis transmembrane conductance regulator) by curcumin: involvement of the keratin 18 network. *J Pharmacol Exp Ther* 2006; 317: 500–505.
19 Melin P, Thoreau V, Norez C, *et al.* The cystic fibrosis mutation G1349D within the signature motif LSHGH of NBD2 abolishes the activation of CFTR chloride channels by genistein. *Biochem Pharmacol* 2004; 67: 2187–2196.
20 Melin P, Hosy E, Vivaudou M, *et al.* CFTR inhibition by glibenclamide requires a positive charge in cytoplasmic loop three. *Biochim Biophys Acta* 2007; 1768: 2438–2446.
21 Norez C, Heda GD, Jensen T, *et al.* Determination of CFTR chloride channel activity and pharmacology using radiotracer flux methods. *J Cyst Fibros* 2004; 3: Suppl. 2, 119–121.
22 Norez C, Antigny F, Noel S, *et al.* A cystic fibrosis respiratory epithelial cell chronically treated by miglustat acquires a non-cystic fibrosis-like phenotype. *Am J Respir Cell Mol Biol* 2009; 41: 217–225.
23 Wu DZ, Yuan JY, Shi HL, *et al.* Palmatine, a protoberberine alkaloid, inhibits both Ca(2+)- and cAMP-activated Cl(-) secretion in isolated rat distal colon. *Br J Pharmacol* 2008; 153: 1203–1213.
24 Best JA, Quinton PM. Salivary secretion assay for drug efficacy for cystic fibrosis in mice. *Exp Physiol* 2005; 90: 189–193.
25 Noel S, Strale PO, Dannhoffer L, *et al.* Stimulation of salivary secretion *in vivo* by CFTR potentiators in Cftr+/+ and Cftr-/- mice. *J Cyst Fibros* 2008; 7: 128–133.
26 Ma T, Thiagarajah JR, Yang H, *et al.* Thiazolidinone CFTR inhibitor identified by high-throughput screening blocks cholera toxin-induced intestinal fluid secretion. *J Clin Invest* 2002; 110: 1651–1658.
27 Muanprasat C, Sonawane ND, Salinas D, *et al.* Discovery of glycine hydrazide pore-occluding CFTR inhibitors: mechanism, structure-activity analysis, and *in vivo* efficacy. *J Gen Physiol* 2004; 124: 125–137.
28 Schultz BD, Singh AK, Devor DC, *et al.* Pharmacology of CFTR chloride channel activity. *Physiol Rev* 1999; 79: Suppl. 1, S109–S144.
29 Norez C, Noel S, Wilke M, *et al.* Rescue of functional delF508-CFTR channels in cystic fibrosis epithelial cells by the α-glucosidase inhibitor miglustat. *FEBS Lett* 2006; 580: 2081–2086.
30 Casals T, Pacheco P, Barreto C, *et al.* Missense mutation R1066C in the second transmembrane domain of CFTR causes a severe cystic fibrosis phenotype: study of 19 heterozygous and 2 homozygous patients. *Hum Mutat* 1997; 10: 387–392.
31 Fanen P, Labarthe R, Garnier F, *et al.* Cystic fibrosis phenotype associated with pancreatic insufficiency does not always reflect the cAMP-dependent chloride conductive pathway defect. Analysis of C225R-CFTR and R1066C-CFTR. *J Biol Chem* 1997; 272: 30563–30566.
32 Mercier B, Lissens W, Novelli G, *et al.* Identification of eight novel mutations in a collaborative analysis of a part of the second transmembrane domain of the CFTR gene. *Genomics* 1993; 16: 296–297.
33 Loo TW, Bartlett MC, Wang Y, *et al.* The chemical chaperone CFcor-325 repairs folding defects in the transmembrane domains of CFTR-processing mutants. *Biochem J* 2006; 395: 537–542.

34 Galietta LJ, Moran O. Identification of CFTR activators and inhibitors: chance or design? *Curr Opin Pharmacol* 2004; 4: 497–503.

35 Kochegarov AA. Pharmacological modulators of voltage-gated calcium channels and their therapeutical application. *Cell Calcium* 2003; 33: 145–162.

36 Whiting PJ. GABA-A receptor subtypes in the brain: a paradigm for CNS drug discovery? *Drug Discov Today* 2003; 8: 445–450.

37 Al Nakkash L, Hwang TC. Activation of wild-type and ΔF508-CFTR by phosphodiesterase inhibitors through cAMP-dependent and -independent mechanisms. *Pflugers Arch* 1999; 437: 553–561.

38 Wang F, Zeltwanger S, Yang IC, *et al.* Actions of genistein on cystic fibrosis transmembrane conductance regulator channel gating. Evidence for two binding sites with opposite effects. *J Gen Physiol* 1998; 111: 477–490.

39 Bulteau L, Derand R, Mettey Y, *et al.* Properties of CFTR activated by the xanthine derivative X-33 in human airway Calu-3 cells. *Am J Physiol Cell Physiol* 2000; 279: C1925–C1937.

40 Haws CM, Nepomuceno IB, Krouse ME, *et al.* ΔF508-CFTR channels: kinetics, activation by forskolin, and potentiation by xanthines. *Am J Physiol* 1996; 270: C1544–C1555.

41 Melin P, Norez C, Callebaut I, *et al.* The glycine residues G551 and G1349 within the ATP-binding cassette signature motifs play critical roles in the activation and inhibition of cystic fibrosis transmembrane conductance regulator channels by phloxine B. *J Membr Biol* 2005; 208: 203–212.